JOURNAL OF MATERIALS SCIENCE 33 (1998) 2653–2658

Cyclic crack growth behaviour of two nickel base turbine disc alloys

G. ARSLAN
Department of Ceramics Engineering, Anadolu University, Yunusemre Campus, 26470 Eskişehir, Turkey

M. DORUK
Department of Metallurgical and Materials Engineering, Middle East Technical University, 06531 Ankara, Turkey

The high temperature fatigue crack growth behaviour of the nickel base superalloys Alloy 718 and René 95 (specimen thickness = 4.1 mm) were investigated and compared with each other. Fatigue crack propagation (FCP) tests were carried out in laboratory air at room temperature and 600 °C by using C-T (compact tension) type specimen that were fatigue precracked at room temperature.

Alloy 718 was found to provide the higher resistance to crack propagation under the present testing conditions.

At 600 °C, in Alloy 718, the fracture path was of mixed type at low and transgranular at high ΔK (stress intensity factor range) values, while it remained intergranular in René 95 throughout the whole ΔK range tested. The difference in the crack growth rates of Alloy 718 with different thicknesses (4.1 mm and 13.0 mm) was related to their different fracture modes.

The striation spacings, both at room temperature and 600 °C, of Alloy 718 were found to be proportional to the empirical equation proposed by Bates and Clark [2] but with a constant of 9.5 instead of 6. However, although the correlation between the microscopic FCP rate obtained from fatigue striation measurements – and hence the empirical equation – and the macroscopic FCP rate was pretty good at room temperature, it was found to be poor at 600 °C, indicating that, at 600 °C, striation formation alone did not control the fatigue resistance of Alloy 718 which is thought to account for the insufficiency of the COD (crack opening displacement) approach to correctly correlate the macroscopic FCP rates of Alloy 718 at these two test temperatures.

1. Introduction

The fatigue crack growth behaviour of Alloy 718 (specimen thickness = 13.0 mm) at 600 °C was investigated previously in the co-operative testing programme of the AGARD Structures and Materials Panel on "High Temperature Cyclic Behaviour of Aerospace Materials" [1].

The present research was planned to shed light on the fracture characteristics of the turbine disc materials Alloy 718 and René 95 (specimen thickness = 4.1 mm) and also to extend the available data about the high temperature crack growth behaviour of these alloys.

Alloy 718 and René 95 are two nickel base superalloys which were developed for a certain number of applications in the gas turbine industry such as the fabrication of turbine discs where the resistance to low cycle fatigue and fatigue crack growth at elevated temperatures are important properties [3]. The highest stresses are experienced in the bore of the disc early in the flight cycle, generally while it is in the temperature range of 200–300 °C. Stresses in the rim region are lower but at higher temperatures, 500–600 °C [4].

The damage tolerance approach differs from the original fail-safe philosophy in that it assumes cracks to exist in the structure already at the very first load cycle. It relies on good non-destructive testing and the accurate prediction of fatigue crack growth lives of components containing cracks using fracture mechanics data. The economic benefits of such an approach have been the driving force for the generation of many of the fatigue crack propagation and threshold data for nickel base alloys, and for the development of turbine disc alloys with improved crack propagation resistance [4].

2. Experimental details

2.1. Testing material and specimen

The materials used for the high temperature fatigue crack propagation (FCP) tests were the wrought

TABLE I Chemical composition of Alloy 718 and René 95 in wt%

Material	Ni	Cr	Nb	Fe	Mo	W	Ti	Al	Co	C
Alloy 718	Bal	18.8	5.1	19.8	3.1	–	1.0	0.5	0.3	0.1
René 95	Bal	14.0	3.8	–	3.5	3.5	2.5	3.5	8.0	0.15

TABLE II Mechanical properties of Alloy 718 and René 95

Material	Temperature (°C)	E (GPa)	σ_y^a (MPa)	UTS (MPa)	Elongation (%)
Alloy 718	25	200	1100	1350	20
Alloy 718	600	165	975	1160	22
René 95	25	225	1310	1620	15
René 95	650	–	1225	1500	14

[a] Yield stress.

nickel–iron base superalloy Alloy 718, and the powder processed nickel base superalloy René 95. All specimens were of C-T type with B (specimen thickness) = 4.1 mm and W (specimen width) = 26.0 mm. The chemical composition and mechanical properties of the alloys are presented in Tables I and II, respectively.

2.2. Testing equipment

The tests were conducted in laboratory air on a creep machine frame that was modified to enable FCP tests to be carried out. A three stage wire wound furnace was adopted and the specimen temperature was controlled to within $\pm 3\,^{\circ}C$.

2.3. Testing procedure

The specimens were fatigue precracked at room temperature by applying load shedding as described by the ASTM standard E 647-83. FCP tests were carried out at room temperature and 600 °C by subjecting the samples to constant load amplitude trapezoidal waves at a cyclic frequency of 0.25 Hz. The load ratio (minimum load/maximum load) employed was 0.1. Crack length was followed on a strip chart recorder by the potential drop technique. A resolution of a 10 μm change in crack length was routinely achieved. The crack growth rate, da/dN, was determined by evaluating the raw data via the seven-point incremental polynomial method given in ASTM standard E 647-83.

As crack front curvature was observed in all of the specimens, a crack curvature correction factor was introduced by averaging five measurements taken at 0, 25, 50, 75, 100% of the specimen width.

3. Results and discussion

Fig. 1 shows the results of the three fatigue crack growth experiments of Alloy 718 with a specimen thickness of 13.0 mm [1]. It indicates that except for the near-threshold region the data of the three experiments coincide with each other. From this figure it is seen that the K_{Ic} (plane strain fracture toughness) value of Alloy 718 under the testing conditions studied lies around 60 MPa m$^{1/2}$.

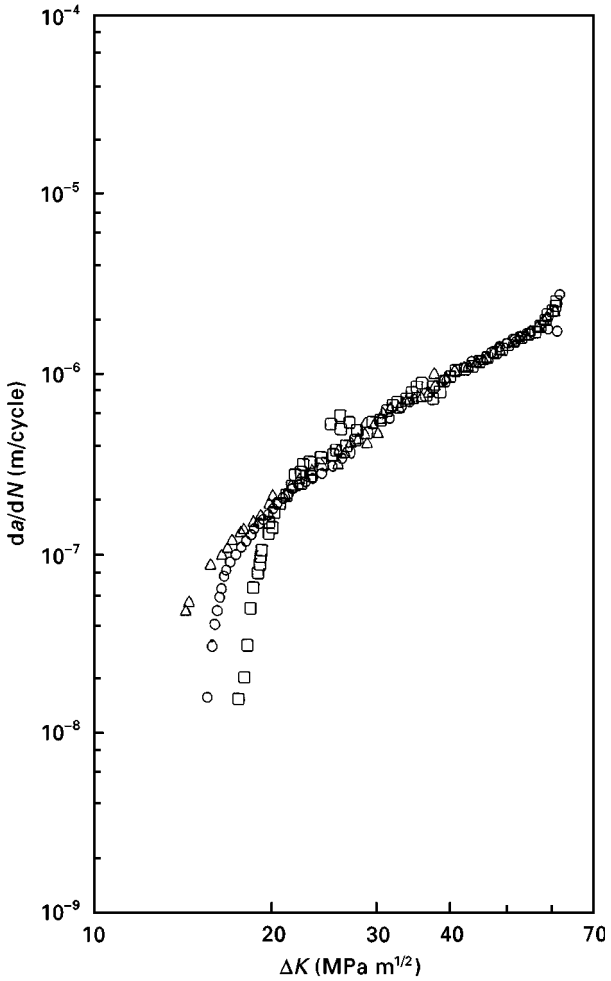

Figure 1 da/dN versus ΔK curves of Alloy 718 specimens (B = 13.0 mm) tested at 600°C. Experiments 1(□) , 2(○) and 3(△).

Fig. 2 shows the effect of temperature on the fatigue crack growth rate curves of Alloy 718 and René 95. It is seen that in both alloys the crack growth rate at a given ΔK is higher at 600 °C than at room temperature except for Alloy 718 in the high ΔK regime. The effect of temperature is shown to be most significant at low ΔK values and to decrease gradually with increasing ΔK. As can be deduced from this figure, increasing the temperature from room temperature to 600 °C affects the crack growth rate of René 95 much more than that of Alloy 718.

It also indicates that, at room temperature, Alloy 718 has a slower crack growth rate than René 95 and that the difference in their resistance to crack propagation becomes increasingly significant with increasing ΔK. The fracture path at room temperature, however, is seen to be of transgranular type in both alloys (Figs 3a and 4a). Therefore, the reason for their different crack growth behaviour at room temperature can not be based on the fact that their modes of crack

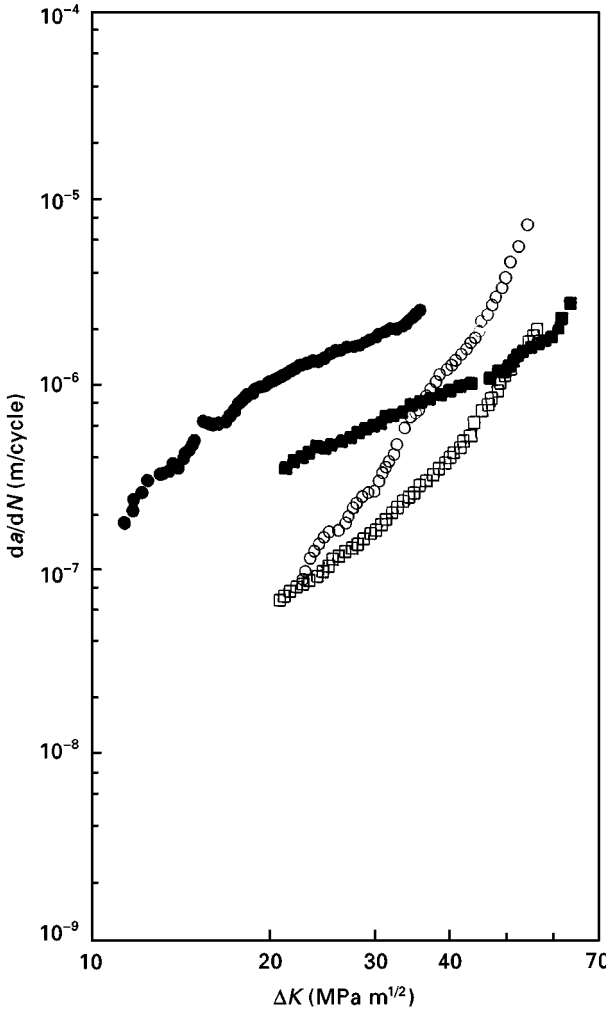

Figure 2 Comparative plot of da/dN versus ΔK curves of Alloy 718 and René 95 specimens ($B = 4.1$ mm) tested at 600 °C and room temperature. (■) Alloy 718, 600 °C; (□) Alloy 718, room temperature; (●) René 95, 600 °C; (○) René 95, room temperature.

propagation are different. However, because the main aim of the research was to study the high temperature behaviour of these alloys no further work was carried out to shed light on this point.

Fig. 2 also compares the fatigue crack growth curves of Alloy 718 and René 95 tested at 600 °C. It is seen that the fatigue crack growth behaviour of René 95 differs significantly from that of Alloy 718. This difference is manifested in Alloy 718 in terms of a slower crack growth rate at a given stress intensity range, and a different mode of fracture path. The crack propagation mode of Alloy 718 is of mixed type at low (Fig. 3b) and transgranular (Fig. 3c) at high ΔK levels while in René 95 the fracture path is intergranular throughout the whole ΔK range tested (Fig. 4b). It could be possible to relate the intergranular fracture path of René 95 to its higher content of carbon and carbide forming alloying elements (Table II) as it is well known that grain boundary carbides play an important role in crack initiation by cracking, by providing sites for void nucleation or by preferential oxidation [5] and also to its lower ductility (Table II), confirming the higher crack growth rate in René 95.

Figs 3h and 4c show the fracture surfaces of Alloy 718 and René 95, respectively, in the fast fracture region. Fracture has advanced by the mechanism of ductile fracture in both alloys. Fig. 3h shows the typical structure of dimples and inclusions in the fast fracture region (Stage 3) of Alloy 718.

To verify whether or not the effect of temperature on crack growth rate of Alloy 718 is the result of the temperature dependence of yield strength and modulus [6] the stress intensity range was normalized with respect to these mechanical properties as is shown in Fig. 5. Because the crack growth rates at different temperatures still differ significantly it follows that the effect of temperature is not at least solely caused by the change in yield strength and modulus with temperature. The change in modulus and yield strength with temperature is less in René 95 than in Alloy 718 ([4], Table II) but the relative increase in crack growth rate larger (Fig. 2). Therefore, the same argument holds for René 95. In fact, if the change in mechanical properties were responsible for the temperature effect, the fracture path should not change upon increasing the temperature, which is in disagreement with Figs 3 and 4 (crack propagation is from bottom to top).

Alternatively, creep and environmentally assisted cracking are both time dependent processes that are thermally activated and may account for the increase in crack growth rate with temperature. To determine whether creep or environment is the dominant time dependent process, crack growth tests in an inert environment must be performed. Such tests could not be accomplished in this research. However, based on the results of Webster [7] and Clavel and Pineau (3), it is concluded that, in Alloy 718, environment is the dominant time-dependent process. The diminishing effect of temperature on crack growth rate of Alloy 718 with increasing ΔK could then be related to the depression of the deleterious effect of the environment which is expected to be most pronounced at low ΔK values [8, 9]. The decreasing contribution of intergranular fracture to crack growth of Alloy 718 with increasing ΔK (compare Fig. 3b and c) and the shift in transition ΔK to unstable fast fracture to higher ΔK values with temperature (Fig. 2) support this view.

In Alloy 718 specimens that were fatigue cracked at 600 °C second phase particles were occassionally found which were identified to be (Ti, Nb) carbonitrides (Fig. 6) and cubic in shape. It is observed that these particles have not fractured at low-to-medium (Fig. 3d) but at high ΔK levels (Fig. 3e). These fractographs also indicate that the incoming particles obstruct the path and force the crack to deflect, thus retarding growth.

Flatter, often striated fracture surfaces are produced when the plastic zone encompasses many grains and several slip systems must be activated within each grain for compatible deformation [4]. These kinds of fatigue striations were easily identified and frequently observed in Alloy 718 both at room temperature and 600 °C (Fig. 3a, f and g) while in René 95 they were observed only at room temperature (Fig. 4a).

James and Mills [10] found striation spacings in Alloy 718 to be in good agreement with the empirical

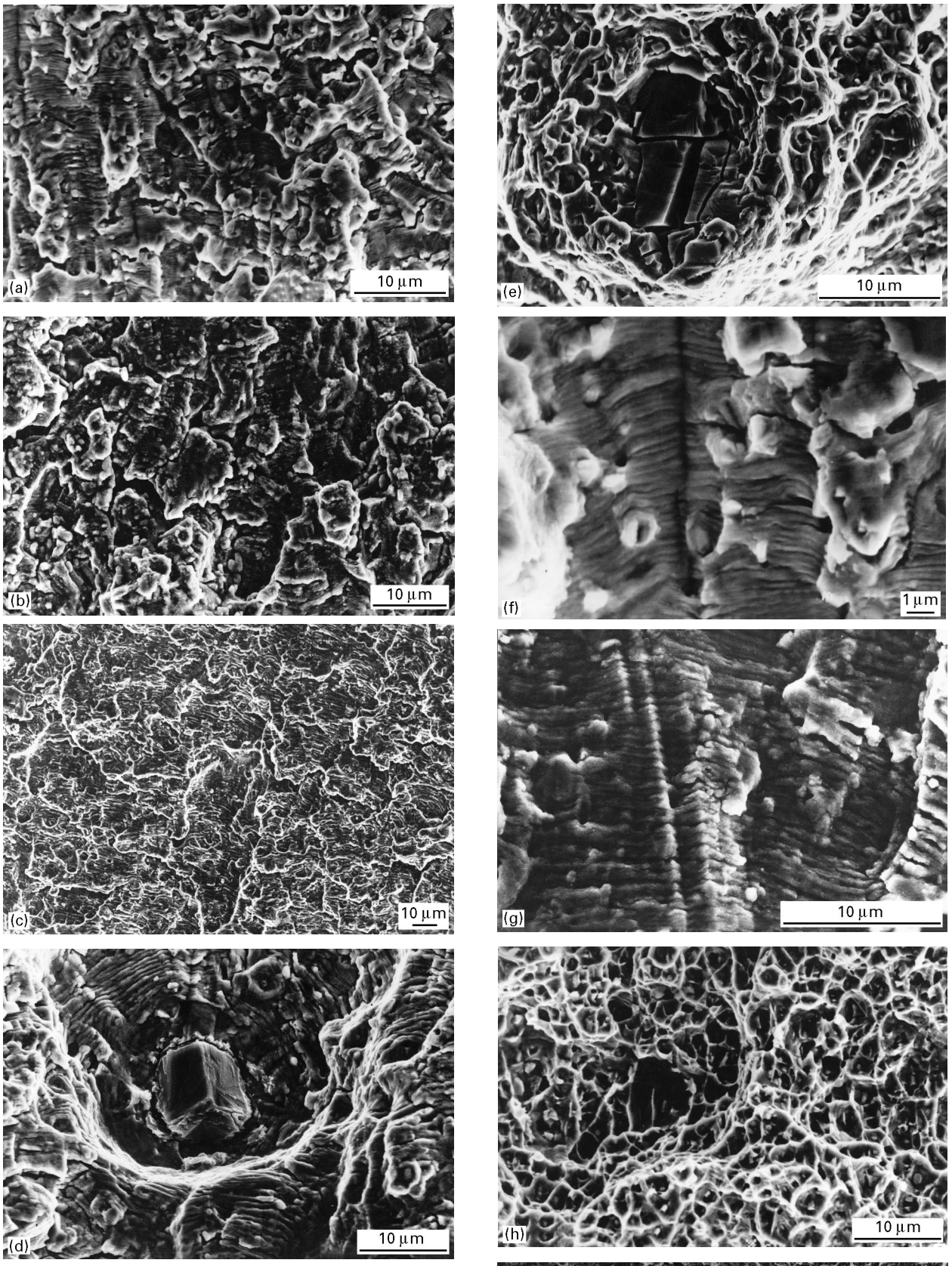

Figure 3 Scanning electron micrographs of Alloy 718 specimens ($B = 4.1$ mm) : (a) T = room temperature, $\Delta K = 35\ \mathrm{MPa\,m^{1/2}}$; (b) $T = 600\ ^{\circ}\mathrm{C}$, $\Delta K = 35\ \mathrm{MPa\,m^{1/2}}$; (c) $T = 600\ ^{\circ}\mathrm{C}$, $\Delta K = 50\ \mathrm{MPa\,m^{1/2}}$; (d) $T = 600\ ^{\circ}\mathrm{C}$, NbC particle, $\Delta K = 30\ \mathrm{MPa\,m^{1/2}}$; (e) $T = 600\ ^{\circ}\mathrm{C}$, NbC particle, $\Delta K = 50\ \mathrm{MPa\,m^{1/2}}$; (f) T = room temperature, $\Delta K = 35\ \mathrm{MPa\,m^{1/2}}$, macroscopic FCP rate = 0.28 μm, microscopic FCP rate = 0.30 μm, FCP rate calculated from the empirical equation = 0.29 μm; (g) $T = 600\ ^{\circ}\mathrm{C}$, $\Delta K = 40\ \mathrm{MPa\,m^{1/2}}$, macroscopic FCP rate = 0.93 μm, microscopic FCP rate = 0.55 μm, FCP rate calculated from the empirical equation = 0.56 μm; (h) T = room temperature, $\Delta K = 60\ \mathrm{MPa\,m^{1/2}}$, (i) $T = 600\ ^{\circ}\mathrm{C}$, $\Delta K = 30\ \mathrm{MPa\,m^{1/2}}$, $B = 13.0$ mm.

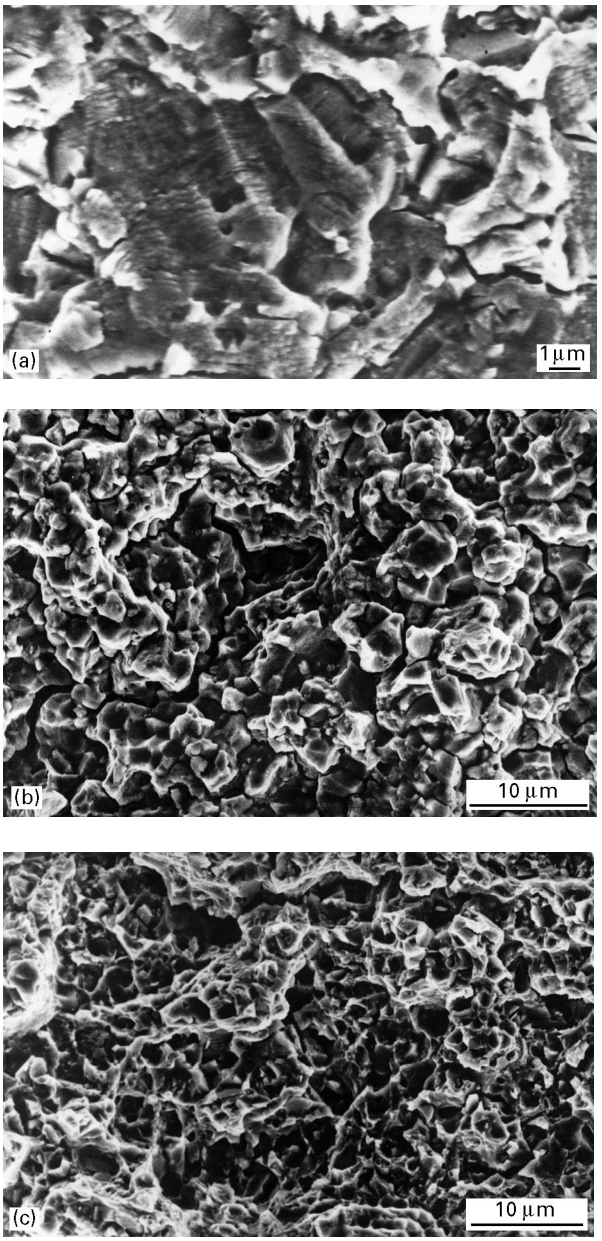

Figure 4 SEM micrographs of René 95 specimens ($B = 4.1$ mm): (a) T = room temperature, $\Delta K = 20\,\mathrm{MPa\,m^{1/2}}$; (b) $T = 600\,^{\circ}\mathrm{C}$, $\Delta K = 30\,\mathrm{MPa\,m^{1/2}}$; (c) T = room temperature, $\Delta K = 55\,\mathrm{MPa\,m^{1/2}}$.

equation proposed by Bates and Clark:

$$\text{striation spacing} = 6(\Delta K/E)^2$$

where ΔK is in $\mathrm{MPa\,m^{1/2}}$ and E (Young's modulus) in GPa, thus giving the striation spacing in μm. In this research the striation spacings in Alloy 718, both at room temperature and 600 °C, were also found to be in agreement with the form of the above equation but with a constant of 9.5 instead of 6. Fig. 5 correlates the crack opening displacement (COD) to the macroscopic FCP rate as the horizontal axis in that figure is effectively proportional to the COD. It indicates that the correlation between the COD approach and the macroscopic FCP rate is poor. A comparison of the microscopic crack growth rates obtained from fatigue striation measurements with the macroscopic FCP rates indicated that, at room temperature, they are in agreement in regime II of the crack growth curve. At 600 °C and in the same ΔK regime, however, the

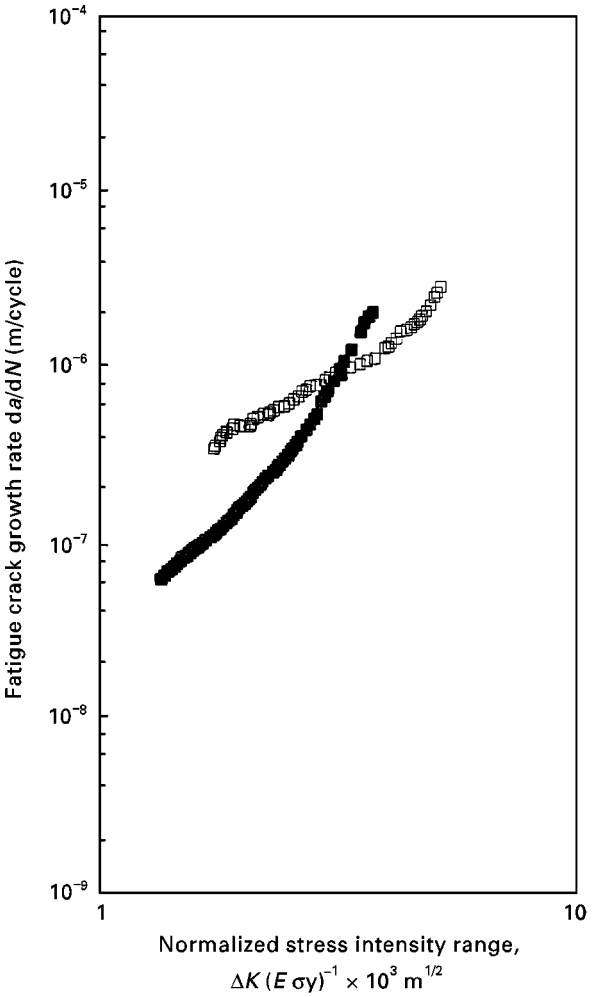

Figure 5 Comparative plot of da/dN versus $\Delta K/\sqrt{E\sigma_{ys}}$ curves of Alloy 718 specimens tested at 600 °C (□) and room temperature (■) ($B = 4.1$ mm).

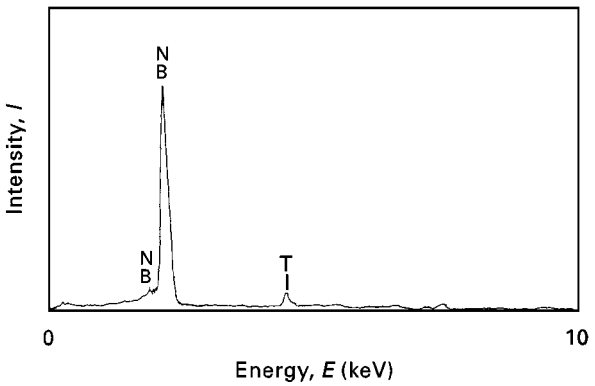

Figure 6 Energy dispersive analysis of particle shown in Fig. 3d.

striation spacings were found to be approximately a factor of two lower than the macroscopic FCP rates. Hence, the empirical equation underestimates the macroscopic FCP rate. Therefore, one can conclude that striation formation alone does not control the fatigue resistance in the ΔK regime under consideration. In the foregoing discussion it was reasoned that it is the environmental interaction which enhances the FCP rate – especially at the lower end of the ΔK spectrum, where in addition to striation formation, intergranular cracking is observed – and thus produces larger increases in FCP rate than the COD approach would indicate.

Thus, although empirical equations might predict striation spacings well, this does not necessarily mean that they also correctly estimate the macroscopic crack growth rate.

Because the material at the surfaces is less constrained from deformation and thus deforms much more readily than that at the centre of the specimen thickness, the crack growth process is slower at the sides. Sadananda and Shahinian [6], who studied the subcritical crack growth behaviour in Alloy 718 under creep conditions, observed somewhat lower crack growth rates at 538 °C on decreasing the thickness which they attributed to either the thickness effect or the fact that the specimens belonged to different heats. At first sight the results of this investigation (Fig. 7) seem to be contrary to the results of Sadananda and Shahinian, as the crack growth rate of the thinner specimen (4.1 mm) is larger at lower ΔK values than that of the thicker one (13 mm). This difference is shown to be significant at the lower end of the ΔK spectrum and to decrease with increasing ΔK (Fig. 7). Both of these findings, however, can be understood if one considers the fact that the fracture path of the thinner specimen is of mixed type (transgranular plus intergranular) at lower ΔK (Fig. 3b) values and transgranular at larger ΔK values (Fig. 3c) in regime II of the crack growth curve. The fracture path of the thicker specimen, on the other hand, is seen to remain transgranular throughout the whole ΔK range (Fig. 3i) in regime II of the crack growth curve. Hence, the crack growth rate of the thinner specimen should be expected to be larger than that of the thicker specimen at the lower end of the ΔK spectrum until a transition in the fracture mode occurs in the former one which is thought to be the result of the decreasing contribution of the environmental effect to crack growth with increasing ΔK.

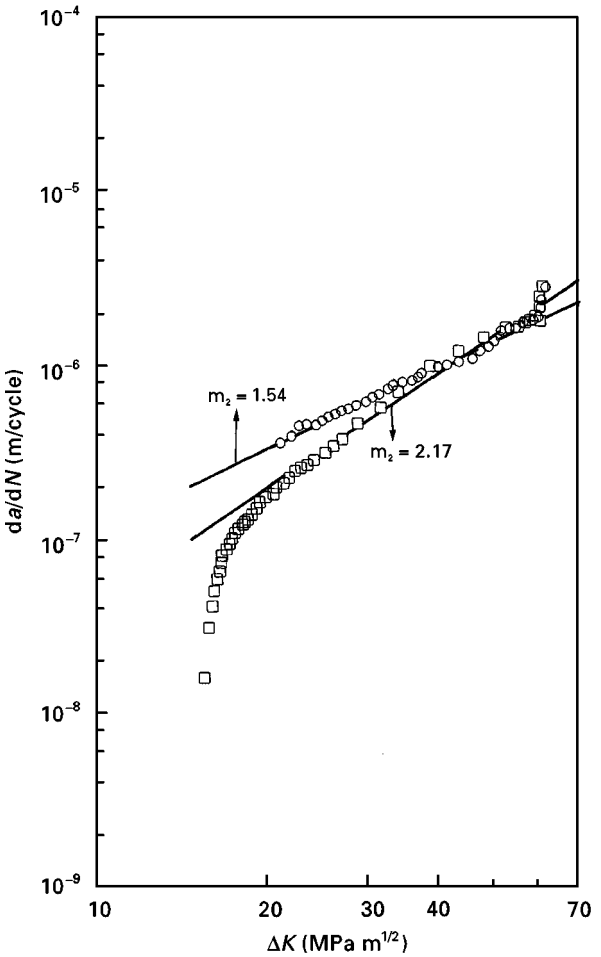

Figure 7 Comparative plot of da/dN versus ΔK curves of Alloy 718 specimens with different thicknesses ($B = 4.1$ mm (□) and $B = 13.0$ mm (○)) tested at 600 °C.

4. Conclusions

The following conclusions can be drawn from the results of this investigation:

1. Alloy 718 when compared with René 95 provides higher resistance to crack propagation under the present testing conditions.
2. At 600 °C, in Alloy 718, the fracture path is of mixed type at low and transgranular at high ΔK values, while it is intergranular in René 95 throughout the whole ΔK range tested. The difference in the crack growth rate of Alloy 718 with different thicknesses is related to their different fracture modes.
3. The striation spacings, both at room temperature and 600 °C, of Alloy 718 (specimen thickness = 4.1 mm) are found to fit to the empirical equation proposed by Bates and Clark, but with a constant of 9.5 instead of 6. However, although the correlation between the microscopic FCP rate – and hence the empirical equation – and the macroscopic FCP rate is good at room temperature, it is found to be poor at 600 °C, indicating that, at 600 °C, striation formation alone does not control the fatigue resistance of Alloy 718 which is thought to account for the insufficiency of the COD approach to correctly correlate the macroscopic FCP rates of Alloy 718 at these two test temperatures.

Acknowledgements

The authors wish to express their thanks to the AGARD Structures and Materials Panel and the TUSAŞ Engine Industry Inc. in Eskişehir, Turkey, for supplying the nickel-base superalloys.

References

1. AGARD-AR-328, Structures and Materials Panel on High Temperature Cyclic Behaviour of Aerospace Materials: Room Temperature Validation Tests of Ti-6Al-4V, published June 1994.
2. R. C. BATES and W. G. CLARK, Jr, *Trans. Quart. ASM* **62** (1969) 380.
3. M. CLAVEL and A. PINEAU, *Met. Trans. A* **9** (1978) 471.
4. J. E. KING, *Mater. Sci. Tech.* **3** (1987) 750.
5. S. D. ANTOLOVICH and N. JAYARAMAN, *Mater. Sci. Engng* **57** (1982) L9.
6. K. SADANANDA and P. SHAHINIAN, *Met. Trans. A* **11** (1980) 267.
7. G. A. WEBSTER, *Mater. Sci. Tech.* **3** (1987) 716.
8. L. A. JAMES, *J. Engng Mater. Technol.* **98** (1976) 235.
9. M. O. SPEIDEL, in "High temperature materials in gas turbines" (Elsevier Scientific Publishing Co., Amsterdam, 1974) p. 207.
10. L. A. JAMES and W. J. MILLS, *Engng Fract. Mech.* **22** (1985) 797.

Received 6 December 1996
and accepted 5 February 1998